

Quantification of metabolically active transient storage (MATS) in two reaches with contrasting transient storage and ecosystem respiration

Alba Argerich,^{1,2} Roy Haggerty,² Eugènia Martí,³ Francesc Sabater,⁴ and Jay Zarnetske²

Received 2 April 2010; revised 1 June 2011; accepted 9 June 2011; published 15 September 2011.

[1] Water transient storage zones are hotspots for metabolic activity in streams although the contribution of different types of transient storage zones to the whole-reach metabolic activity is difficult to quantify. In this study we present a method to measure the fraction of the transient storage that is metabolically active (MATS) in two consecutive reaches with contrasting hydrological and biological characteristics. We used combined additions of resazurin (Raz) and Cl in a reach scoured to bedrock and in a reach containing a deep alluvial deposit. The MATS zones measured 0.002 m² in the bedrock reach (37% of transient storage) and 0.291 m² in the alluvial reach (100% of transient storage). The effective rate coefficient of Raz transformation in the MATS of the bedrock reach was approximately 16 times that of the alluvial reach. However, when we take into account the contribution of the MATS zone to overall metabolic activity, Raz transformation in the MATS zone was 2.2 times slower in the bedrock reach than in the alluvial reach. The difference was similar to the difference in ecosystem respiration, which was 1.8 times lower in the bedrock reach than in the alluvial reach, suggesting that the MATS zones were important contributors to ecosystem respiration. Results indicate that the quantification of MATS can improve our understanding of the role that transient storage zones play on stream metabolic processes and demonstrate the utility of Raz as a “smart” tracer that provides new information on metabolic activity at a whole-reach and at smaller scale.

Citation: Argerich, A., R. Haggerty, E. Martí, F. Sabater, and J. Zarnetske (2011), Quantification of metabolically active transient storage (MATS) in two reaches with contrasting transient storage and ecosystem respiration, *J. Geophys. Res.*, 116, G03034, doi:10.1029/2010JG001379.

1. Introduction

[2] Transient storage in streams occurs at locations where water moves at slower velocity than the average channel velocity, and thus, in these zones, water residence time tends to be longer than in the free-flowing water of the stream channel [Bencala and Walters, 1983]. Quantification of these zones has become a critical issue in biogeochemical studies of stream ecosystems, in particular, in those examining spatial or temporal variation in nutrient retention [e.g., Butturini and Sabater, 1999; Bukaveckas, 2007; Argerich et al., 2008] or metabolism [Mulholland et al., 2001]. It is expected that larger transient storage may enhance the interaction between dissolved nutrients and microbial communities and, thus, increase nutrient uptake and metabolism at the whole reach scale [Fellows et al., 2006]. However, while some

studies support a positive relationship between nutrient uptake or metabolism and size of transient storage [Valett et al., 1996; Mulholland et al., 2001; Ensign and Doyle, 2005], others indicate a lack of consistent relationships [Webster et al., 2003; Simon et al., 2005]. One of the reasons for this inconsistency may stem from the limitations of conservative hydrologic tracers, which cannot distinguish among the different stream compartments that contribute to transient storage (e.g., hyporheic zone versus surface flow eddy), even though biogeochemical processes may differ among them. Only a few attempts have been made to distinguish among compartments that contribute to transient storage. Most of them separate the transient storage zones based on their physics and location (e.g., surface versus hyporheic [Gooseff et al., 2005; Phanikumar et al., 2007; Zarnetske et al., 2007; Briggs et al., 2009]), and only a few studies separate them based on their metabolic characteristics [Harvey and Fuller, 1998; Fuller and Harvey, 2000; Fellows et al., 2001; Gooseff et al., 2004]. However, they did not always are able to quantify the contribution of each compartment to the overall transient storage.

[3] In this study, we used an alternative philosophical approach to quantify, characterize, and distinguish between transient storage zones. We distinguish metabolically active

¹Departament d'Ecologia, Universitat de Barcelona, Barcelona, Spain.

²Department of Geosciences, Oregon State University, Corvallis, Oregon, USA.

³Biogeodynamics and Biodiversity Group, Centre d'Estudis Avançats de Blanes, Blanes, Spain.

⁴Departament d'Ecologia, Universitat de Barcelona, Barcelona, Spain.

transient storage (MATS) from a less-active or “metabolically inactive” transient storage (MITS). We used resazurin (hereafter referred to as Raz) as a “smart” tracer, the transformation of which is a proxy for metabolic activity [Haggerty *et al.*, 2008, 2009]. Raz is a weakly fluorescent phenoxazine dye that undergoes an irreversible reduction to highly fluorescent resorufin (hereafter referred to as Rru) in the presence of aerobic respiration [Karakashev *et al.*, 2003; McNicholl *et al.*, 2007]. Haggerty *et al.* [2008] characterized the decay, sorption, transformation, and transport of Raz and Rru in water and saturated stream sediment. That study showed that Raz and Rru do not react or degrade in stream water alone, but that Raz does transform quickly (Raz to Rru rate coefficient = 1.4 h^{-1}) to Rru in colonized stream sediment. Both Raz and Rru photodegrade, but not sufficiently to pose a problem except in the brightest sunlight or over travel times of multiple hours in normal daylight. These results suggested that Raz could be a suitable tracer to help characterize MATS. More recently, Haggerty *et al.* [2009] tested Raz as a MATS-sensitive tracer under field conditions by conducting an injection in a headwater stream and analyzing Raz and Rru transformation at the reach scale. Results showed that Raz to Rru transformation was proportional to dissolved oxygen (DO) consumption in the hyporheic zone and moderately correlated to whole-reach instantaneous respiration rates. However, Haggerty *et al.* [2009] worked in a relatively homogeneous reach and made no attempt to quantify the fraction of transient storage that was metabolically active.

[4] Our objective is to quantify the MATS in two reaches that are different in terms of transient storage and which we hypothesize are different in MATS. Previous studies have shown that the hyporheic zone can contribute a substantial proportion of whole-stream respiration [Grimm and Fisher, 1984; Mulholland *et al.*, 1997; Fellows *et al.*, 2001]. Therefore, we hypothesized MATS would be greater in an alluvial reach than in a bedrock reach of the same stream. At the same time, we wanted to know what fraction of the transient storage in these two reaches was metabolically active; i.e., what is the MATS fraction? Furthermore, we wanted to know how the rates of metabolism in the MATS compared between the reaches; e.g., while it was expected that the alluvial reach would have greater metabolism, would the rate of metabolism within zones identified as MATS be larger or smaller in the alluvial reach?

[5] To answer these questions, we needed to develop a parameter estimation method for Raz transformation and MATS. OTIS-P [Runkel, 1998], although well-known among stream ecologists, does not allow the inclusion of coupled reactions, in contrast to STAMMT-L [Haggerty and Reeves, 2002] which can handle coupled reactions, and has been applied before in field experiments with Raz [Haggerty *et al.*, 2009]. However, STAMMT-L does not handle two sub-reaches with different conditions. Therefore, we decided to estimate the hydraulic parameters with OTIS-P and to use the temporal moments of the breakthrough curves (BTC) to estimate reaction parameters without solving the transport equations directly [Wörman, 2000; Schmid, 2003].

2. Study Site

[6] We worked in WS03, a steep, second-order stream located in the H.J. Andrews Experimental Forest in the

western Cascade Mountains of Oregon ($44^{\circ}10'N$, $122^{\circ}15'W$; Figure 1). The stream drains a 1 km^2 catchment forested with ~ 32 year old Douglas fir (*Pseudotsuga menziesii*), western hemlock (*Tsuga heterophylla*), and western red cedar (*Thuja plicata*) away from the stream and ~ 11 year old red alder (*Alnus rubra* Bong.) and willow (*Salix* spp.) in the riparian zone [Kasahara and Wondzell, 2003]. The climate is characterized by wet, mild winters and dry, cool summers. Mean monthly atmospheric temperature ranges from 1°C in January to 18°C in July. Precipitation is concentrated in autumn and winter and averages 2300 to 3550 mm yr^{-1} depending on the elevation. Annual stream low flows occur at the end of the summer dry season, with discharge $< 3 \text{ L s}^{-1}$. The Raz experiment was conducted on 17–18 September 2007 and discharge, measured at the WS03 stream gauge (operated by the H. J. Andrews Experimental Forest and located 127.1 m downstream of our last sampling site S20; Figure 1), was 1.61 L s^{-1} .

[7] For this study we considered two consecutive reaches shown in Figure 1. The upstream reach (hereafter referred to as the bedrock reach; SE quadrant of map) was 357.5 m long and was scoured to bedrock by debris flows in the winters of 1964–1965 and 1995–1996. This reach has a slope of 0.16 m m^{-1} , and cascade-pool morphology with some shallow and sparse alluvium in pools along the last 133 m (downstream of the surface sampling point S7). The downstream reach (hereafter referred to as the alluvial reach; NW quadrant of map) was 205.7 m long and was characterized by a deep alluvium deposit created by the deposition of the debris flows. This reach has a slope of 0.14 m m^{-1} and step-pool morphology. A small tributary joins the WS03 main stem at the downstream end of the bedrock reach. Haggerty *et al.* [2002], Johnson [2004], Gooseff *et al.* [2005], and Wondzell [2006] performed tracer and heat experiments in these reaches. These earlier studies showed that transient storage in the bedrock reach is confined to the surface channel with a small area of exchange but exhibits rapid water exchange with the main channel. Conversely, the alluvial reach has a larger transient storage zone which is located in both the surface channel and the hyporheic zone and exhibits slow water exchange with the main channel.

3. Methods

3.1. Stream Tracer Injection

[8] The experiment consisted of a constant rate injection of a solution of 36.8 g of Raz and 3.7 kg of NaCl in 139 L of stream water using a Masterflex (Vernon Hills, Illinois) L/S battery-powered peristaltic pump at a rate of 123 mL min^{-1} . The solution was injected at the head of the bedrock reach starting at 16:00 LT on 17 September 2007 and lasted for 17.3 h (i.e., until 09:20 LT the next day). Electrical conductivity (EC), as a surrogate for Cl concentrations [Wondzell, 2006], was automatically recorded every 5 minutes at the end of each reach (i.e., S12 and S20 in Figure 1) using a Hydrolab Water Quality Multiprobe (model MiniSonde 5; Hach Company, Loveland, Colorado). EC was also measured at 1 minute intervals in 11 wells located in the alluvial reach (Figure 1) using 11 EC-probes connected via a multiplexer to a CR1000 data logger (Campbell Scientific, Logan, Utah). Wells were located near to the end of the alluvial reach (i.e., surface sampling site S20, Figure 1) and

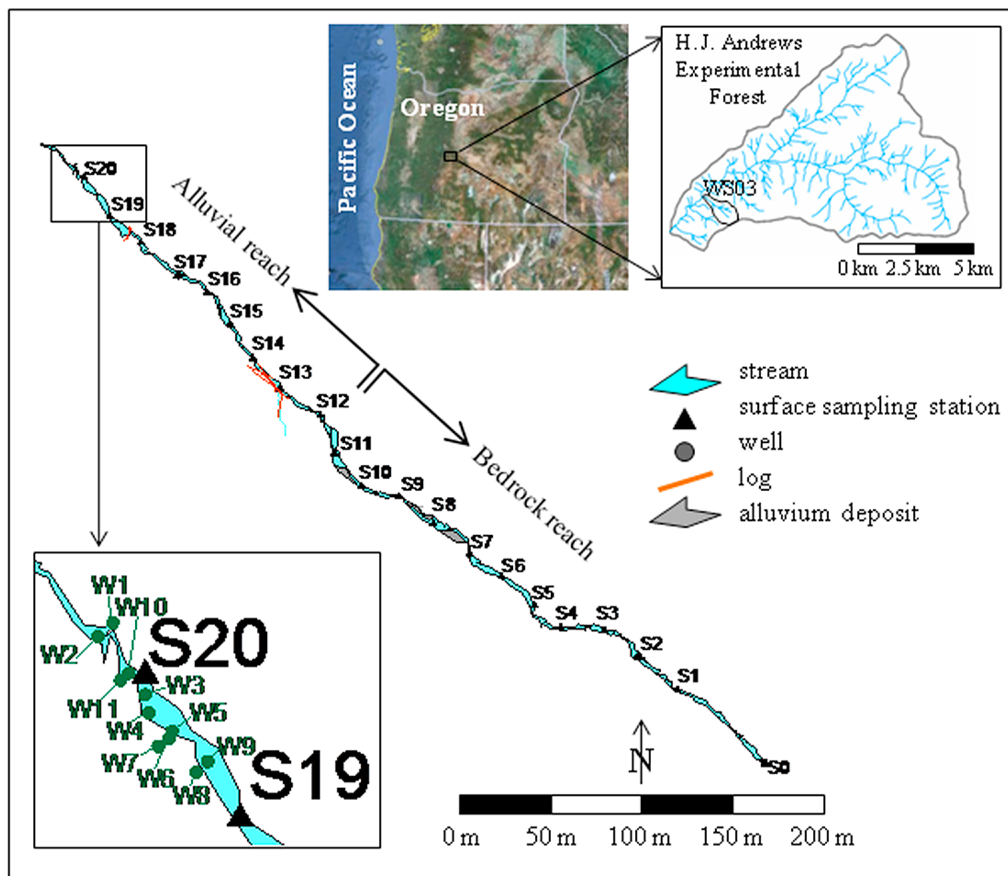


Figure 1. Map of the study section at the watershed 3 of the H. J. Andrews Experimental in the western Cascade Mountains of Oregon ($44^{\circ}10'N$, $122^{\circ}15'W$). Data for this map were surveyed on 24–27 September 2007. The two study reaches and the location of the tributary input are shown. Direction of water flow is from bottom right to top left. Point of solute injection and the location of sampling stations for surface water along the reaches are indicated with S0 to S20 symbols. The inset provides the detailed location of the 11 wells (W1 to W11).

were installed by S. Wondzell in the summer of 1997. Wells consisted of 3.18-cm diameter schedule 40 PVC tubes screened over the lower 50 cm [Kasahara and Wondzell, 2003; Wondzell, 2006].

[9] Water samples for the analysis of Raz and Rru concentrations were collected over time at the downstream end of the two reaches (i.e., S12 and S20) using two ISCO autosamplers (Teledyne Isco 3700 portable sampler, Lincoln, Nebraska). Sample frequency was accommodated to changes in EC and lasted until 65 h after the start of the injection.

[10] To characterize the longitudinal profile of EC, Raz and Rru concentrations, EC measurements and water samples were collected before the injection began (i.e., background concentration) and just before stopping the injection (i.e., plateau concentration) at 20 surface sampling sites spaced approximately 25 m along the thalweg of the reaches (Figure 1) and at the 11 wells. Water samples were filtered through Whatman (Kent, United Kingdom) GF/F glass-fiber filters ($0.7\ \mu\text{m}$ pore size), stored in the dark and refrigerated at 4°C until analysis. Once in the laboratory, and because Raz and Rru fluorescence is constant above pH 8 but decrease sharply at $\text{pH} < 6.5$, samples were buffered to pH

8 prior to fluorescence analysis and processed following Haggerty *et al.* [2008].

3.2. Physical Characterization of the Reaches

[11] The stream topography and surface water elevations were surveyed on 24 to 27 September 2007 using a Topcon GTS 223 total station (Figure 1). During the topographic survey, the stream discharge was the same as during the tracer experiment. Stream left and right edges were located at every site that differed by more than approximately 5 cm vertically and horizontally from any adjacent site. We recorded the locations of all sampling stations, logs and other elements present in the channel. In total, approximately 500 topographic points were collected to define the banks. Data obtained from the survey was used to calculate the slope and average wet width of the two sub-reaches.

[12] We measured discharge (Q , L s^{-1}) and average water velocity (u , m s^{-1}) using the time-curve EC data recorded at S12 and S20. We calculated u by dividing the distance between the injection point and the sampling station by the time needed to increase the EC to one half of the plateau (i.e., nominal travel time). We calculated Q based on a tracer

mass balance approach [Shaw, 1994] assuming a total recovery of the conservative tracer injected.

3.3. Measurement of Ecosystem Respiration

[13] Daily ecosystem respiration (ER, g O₂ m⁻² d⁻¹) in the two reaches was estimated using the upstream-downstream dissolved oxygen (DO, mg O₂ L⁻¹) change technique [Bott, 2006]. Concentration of DO and temperature were recorded at 5-min intervals beginning at sunset (19:20 LT) and continuing over night for 6.5 h (01:35 LT) with two Hydrolab Water Quality Multiprobes (model MiniSonde 5; Hach Company, Loveland, Colorado). Measurements were done on the day prior to the injection at the bedrock reach (DO probes located at S0 and S12) and simultaneously with the injection experiment at the alluvial reach (DO probes located at S12 and S20). Percent DO saturation was estimated using DO concentration and temperature data together with a standard altitude-air pressure algorithm to correct for site altitude. The reaeration rate coefficient (k) at each reach was estimated based on the nighttime regression method [Young and Huryn, 1996]. Instantaneous ER rates (flux units of g O₂ m⁻² d⁻¹) were calculated during night-time by subtracting the DO difference between output and input from the DO added across the water surface by reaeration, and dividing by bed area:

$$ER = \frac{Q}{wL} [k_2 Def t_n - (DO_{down} - DO_{up})] \times \frac{3600 \times 24}{1000} \quad (1)$$

where Q is discharge in L s⁻¹, w is the average wetted width of the reach, L is the distance between the two stations, k_2 is the reaeration rate coefficient adjusted to streamwater temperature at each sampling time calculated using the *Elmore and West* [1961] equation, Def is the average DO saturation deficit in the reach, t_n is the nominal travel time between upstream and downstream, and DO_{down} and DO_{up} are oxygen concentration downstream and upstream of the reach, respectively. Daily rates of ER were calculated as the absolute value of the average of the instantaneous ER rates measured during night-time extrapolated to 24 h.

3.4. Surface Versus Hyporheic Raz Transformation

[14] By the end of the injection, the alluvial reach did not achieve plateau conditions. Therefore, the water that entered the hyporheic zone from the surface had different concentrations of Raz and Rru over time. To examine if the hyporheic Raz and Rru concentrations were significantly different than those in surface water, we compared Raz and Rru concentrations in the wells at time t to those measured at the nearest surface sampling point (i.e., S20) at the time when the water entered the subsurface, $t - t_m^{well} + t_m^{surf}$, where t_m^{well} is the minimum travel time between the head of the alluvial reach and the well, t_m^{surf} the minimum travel time between the head of the alluvial reach and S20. The equation is

$$\Delta C_{well,t}^{exp} = \Delta C_{S20}^{obs} (t - t_m^{well} + t_m^{surf}) \times SW \quad (2)$$

where $\Delta C_{well,t}^{exp}$ is the expected concentration in the well (assuming no transformation), $C_{S20}^{obs} (t - t_m^{well} + t_m^{surf})$ is the observed concentration in surface water and SW is the percentage of surface water that reached the well at the time of plateau sampling (t). SW was calculated as the increase in

EC at wells between time t and $t = 0$ (i.e., measured EC at pre-injection conditions) relative to the increase observed at surface water at the beginning of the alluvial reach between the time that water potentially entered to the hyporheic zone (i.e., time = $t - t_m^{well}$) and $t = 0$.

$$SW = \frac{EC_{well}(t) - EC_{well}(t = 0)}{EC_{S12}(t - t_m^{well}) - EC_{S12}(t = 0)} \quad (3)$$

where t_m^{well} was calculated from the first arrival time [Triska *et al.*, 1989].

3.5. Governing Equations

[15] The mass balance equation for transport of a conservative tracer with advection, dispersion, and transient storage is [Bencala and Walters, 1983]

$$\frac{\partial C}{\partial t} = -\frac{Q}{A} \frac{\partial C}{\partial x} + \frac{1}{A} \frac{\partial}{\partial x} \left(AD \frac{\partial C}{\partial x} \right) - \frac{A_s}{A} \alpha_2 (C - S) \quad (4)$$

$$\frac{\partial S}{\partial t} \alpha_2 (C - S) \quad (5)$$

where C and S are solute concentrations ($\mu\text{g L}^{-1}$) in the main channel and in the storage zone, respectively; A and A_s (m²) are the cross-sectional areas of the main channel and the transient storage zone, respectively; D is the dispersion coefficient (m² s⁻¹), Q is discharge (L s⁻¹), t is time (s), x is distance (m), and α_2 (s⁻¹) is the inverse of mean residence time in transient storage. The parameter a_2 equals aA/A_s , where a is the storage zone exchange coefficient (s⁻¹) of Bencala and Walters [1983] and many others [e.g., Runkel, 1998].

[16] For reactive solutes, such as Raz and Rru, we need to add decay and transformation in the metabolically active transient storage (MATS) fraction (f). The equations, following Haggerty *et al.* [2009] and including the MATS fraction (f), are

$$\begin{aligned} \frac{\partial C_{Raz}}{\partial t} = & -\frac{Q}{A} \frac{\partial C_{Raz}}{\partial x} + \frac{1}{A} \frac{\partial}{\partial x} \left(AD \frac{\partial C_{Raz}}{\partial x} \right) \\ & - \frac{A_s}{A} \alpha_2 [C_{Raz} - f S_{Raz}^a - (1-f) S_{Raz}^i] - \lambda_1 C_{Raz} \end{aligned} \quad (6)$$

$$\frac{\partial S_{Raz}^a}{\partial t} = \alpha_2 (C_{Raz} - S_{Raz}^a) - \lambda_1^a S_{Raz}^a \quad (7)$$

$$\frac{\partial S_{Raz}^i}{\partial t} = \alpha_2 (C_{Raz} - S_{Raz}^i) - \lambda_1^i S_{Raz}^i \quad (8)$$

$$\begin{aligned} \frac{\partial C_{Rru}}{\partial t} = & -\frac{Q}{A} \frac{\partial C_{Rru}}{\partial x} + \frac{1}{A} \frac{\partial}{\partial x} \left(AD \frac{\partial C_{Rru}}{\partial x} \right) \\ & - \frac{A_s}{A} \alpha_2 [C_{Rru} - f S_{Rru}^a - (1-f) S_{Rru}^i] \\ & - \lambda_2^i C_{Rru} + \lambda_1^i y^i C_{Raz} \end{aligned} \quad (9)$$

$$\frac{\partial S_{Rru}^a}{\partial t} = \alpha_2 (C_{Rru} - S_{Rru}^a) - \lambda_2^a S_{Rru}^a + \lambda_1^a y^a S_{Raz}^a \quad (10)$$

$$\frac{\partial S_{Rru}^i}{\partial t} = \alpha_2 (C_{Rru} - S_{Rru}^i) - \lambda_2^i S_{Rru}^i + \lambda_1^i y^i S_{Raz}^i \quad (11)$$

where superscript “a” refers to the metabolically active transient storage (MATS) zone, superscript “i” refers to the metabolically inactive transient storage zone, λ_1 is the sum of Raz decay rate coefficient and Raz to Rru transformation rate coefficient (h^{-1}), λ_2 is Rru decay rate coefficient (h^{-1}), and f is the MATS fraction. Other variables and parameters are defined in the notation section.

3.6. Parameter Estimation

[17] We used OTIS-P [Runkel, 1998] to estimate the dispersion coefficient (D), channel cross-sectional area (A), channel storage zone cross-sectional area (A_s/A), and storage zone exchange coefficient (a) from the BTC of EC.

[18] To determine whether the length of the reach was suitable for estimating transient storage parameters we calculated Damköhler values (DaI) [Wagner and Harvey, 1997]:

$$DaI = \frac{\alpha(1 + A/A_s)L}{u} \quad (12)$$

where L is reach length. When DaI is >1 , the length of the study reach is too long so there is nearly complete solute transfer between the main channel and storage zone. When the DaI is <1 , very little solute enters the storage zone [Harvey and Wagner, 2000]. Ideal values of DaI should be ~ 1.0 but values between 0.5 and 5.0 are reasonable [Harvey and Wagner, 2000]. Additionally, we calculated the fraction of the median travel time attributable to transient storage for a standardized length of 200 m (F_{med}^{200}) [Runkel, 2002] using

$$F_{med}^{200} = \left[1 - e^{-L(\alpha/u)}\right] \frac{A_s}{A + A_s} \quad (13)$$

To estimate the other parameters, we compared the temporal moments of the breakthrough data to the moments calculated with the model (equations (4)–(11)). The model moments can be derived with the Laplace transform of the model and can be calculated without having to solve the equations themselves [e.g., Aris, 1958; Kučera, 1965; Goltz and Roberts, 1987; Schmid, 2003; Wörman and Wachniew, 2007]. Temporal moments are defined as

$$m_n = \int_0^{\infty} t^n C(x, t) dt \quad (14)$$

where m_n is the n th temporal moment at a location x and at a time t . The zeroth moment is the area under the breakthrough curve and the first moment is the zeroth moment multiplied by the mean arrival time. Several properties of the moments are very useful and commonly used in hydrology. The most important property is that the zeroth moment of a conservative solute is independent of exchange with the transient storage zone, while the zeroth moment of a reacting solute is dependent on both exchange and reaction rates. Another property is that the mean arrival time of a conservative solute depends on the ratio A_s/A (expressed as β below to save space), but not on the rate of exchange with the transient storage zone [Harvey and Gorelick, 1995]. To keep the equations for reactive solutes reasonably simple, we set $D = 0$. While D does not have a large influence on the zeroth or first moments, it has a significant influence on the second moment. Therefore, the analyses that follow are based only on the zeroth and first moments. We then compared the

moments from the breakthrough data to the theoretical moments predicted using the model (equations (4)–(11)).

[19] The mean travel time (τ , h) between any upstream (superscript u) and any downstream (superscript d) sampling point can be calculated from the temporal moments at the upstream and downstream sampling points as [Sardin et al., 1991]

$$\tau = \frac{m_{1,EC}^d}{m_{0,EC}^d} - \frac{m_{1,EC}^u}{m_{0,EC}^u} = t_n(1 + \beta) \quad (15)$$

The mean travel time of a reacting solute is dependent on exchange and reaction rates. Therefore, for a reactive tracer such as Raz, the mean travel time is

$$\tau_{Raz} = \frac{m_{1,Raz}^d}{m_{0,Raz}^d} - \frac{m_{1,Raz}^u}{m_{0,Raz}^u} = t_n \left(1 + (1-f)\beta + \frac{f\alpha_2^2\beta}{(\alpha_2 + \lambda_1^a)^2} \right) \quad (16)$$

The relationship between upstream and downstream temporal moments for EC are

$$m_{0,EC}^d = m_{0,EC}^u \quad (17)$$

$$m_{1,EC}^d = m_{1,EC}^u + m_{0,EC}^u(1 + \beta)t_n \quad (18)$$

The relationship between upstream and downstream temporal moments for Raz are:

$$m_{0,Raz}^d = m_{0,Raz}^u e^{-L/S_{w-Raz}} \quad (19)$$

$$m_{1,Raz}^d = \left[m_{1,Raz}^u + m_{0,Raz}^u t_n \left(1 + \frac{\alpha_2^2\beta}{(\alpha_2 + \lambda_1^a + \lambda_1^i)^2} \right) \right] e^{-L/S_{w-Raz}} \quad (20)$$

The uptake length (S_w , m), defined as the average distance travelled by a reactive molecule before decay or transformation, can be considered as a measure of the reach efficiency in processing reactive solutes [Stream Solute Workshop, 1990]. There are several ways to calculate S_w , depending on the complexity of the system. The simplest one assumes that solutes are transported by advection only (mixing due to dispersion – i.e., $D = 0$, and transient storage does not occur) and uptake takes place only in the main channel [Stream Solute Workshop, 1990]. In this study, transient storage plays an important role in reactive solute processing so we included it in the S_w for Raz. This case, which is consistent with, but expanded from, the S_w type II of Runkel [2007] (who also assumed $D = 0$), yields

$$S_{w-Raz} = \frac{Q}{A} \left(\lambda_1^i + \beta f \frac{\alpha_2 \lambda_1^a}{\alpha_2 + \lambda_1^a} + \beta(1-f) \frac{\alpha_2 \lambda_1^i}{\alpha_2 + \lambda_1^i} \right)^{-1} \quad (21a)$$

Note that there are three terms that contribute to the transformation of Raz, which are, from left to right within the outer parentheses: (1) transformation in the channel; (2) transformation in MATS; and (3) transformation in MITS. We can define an effective reaction rate coefficient for MATS,

$$\lambda_e^a = \frac{\alpha_2 \lambda_1^a}{\alpha_2 + \lambda_1^a} \quad (21b)$$

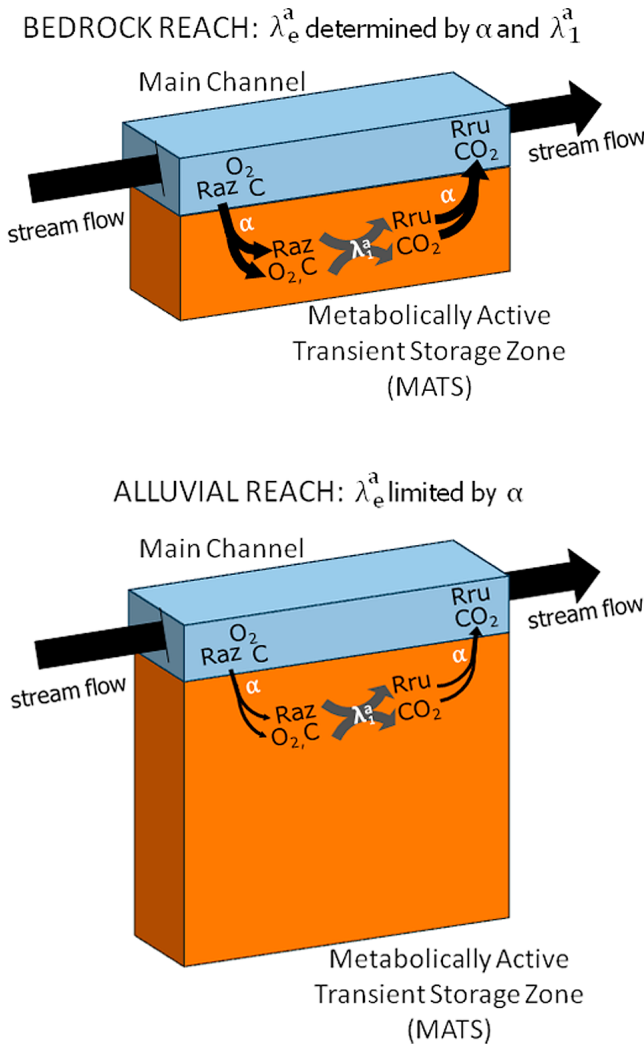


Figure 2. Conceptual illustration of the main channel and the MATS zone of the reaches under study. The water exchange coefficient between the two compartments (α) influence the supply of oxygen, Raz, and other metabolites needed for aerobic respiration to the MATS zone. The effective reaction rate coefficient (λ_e^a) for metabolic activity in the MATS zone results from the interaction of hydrology (α) and biology (λ_e^a).

and a volume-weighted effective reaction rate coefficient, $\beta f \lambda_e^a$, that corrects the reaction rate coefficient by the relative size of the metabolically active transient storage, i.e., the reaction rate coefficient when we take into account the contribution of the MATS zone to overall metabolic activity. MITS also has an effective reaction rate coefficient and a volume-weighted effective reaction rate coefficient of the same form.

[20] Equation (21a) can be re-written with the effective reaction rate coefficients:

$$S_{w-Raz} = \frac{Q}{A} (\lambda_1^a + \beta f \lambda_e^a + \beta(1-f)\lambda_e^i)^{-1} \quad (22a)$$

where λ_e^a is the effective reaction rate coefficient in the MATS [h^{-1}], and λ_e^i is the effective reaction rate coefficient in the MITS [h^{-1}]. In most circumstances (where transformation in the water column is slow relative to transformation in the benthos and hyporheos), we expect the following simplification for Raz to be valid:

$$S_{w-Raz} = \frac{Q}{A\beta f \lambda_e^a} = \frac{u}{\beta f \lambda_e^a} \quad (22b)$$

That is, the uptake length is the velocity divided by the volume-weighted effective reaction rate coefficient of the MATS zone.

[21] An important point is that the effective reaction rate coefficient λ_e^a encompasses the combined consequences of hydrology and biology on Raz transformation (which is a proxy for aerobic metabolism). When exchange is very fast relative to reaction, $\lambda_e^a \cong \lambda_1^a$, then stream metabolism is controlled by biology (which, in turn, could be controlled by other factors such as nutrients, grazing pressure, or temperature). However, when exchange is slow relative to reaction, $\lambda_e^a \cong \alpha$, the stream metabolism is limited by the hydrologic supply of oxygen and nutrients, i.e., is limited by hydrology (Figure 2).

[22] The uptake length can be calculated from the data from a short injection (non-plateau) using the upstream and downstream temporal moments (equation (19)), which was implicitly conjectured by Tank *et al.* [2008] in the use of pulse injections to measure uptake length, and which can be proven using temporal moments:

$$S_{w-Raz} = - \frac{L}{\ln(m_{0,Raz}^d / m_{0,Raz}^u)} \quad (23)$$

Uptake velocity, (the average velocity at which reactive solutes are transferred to the benthos; V_f , $mm \text{ min}^{-1}$) can then be calculated by dividing u times h by S_w [*Stream Solute Workshop*, 1990].

[23] To calculate decay and reaction rates in the MATS zone we assumed decay and reaction rates in the main channel and in the MITS to be equal to those obtained experimentally by Haggerty *et al.* [2008] in stream water. Decay and reaction rates were measured in stream water (see notation section) and found to be very low in comparison to values observed in sediments.

[24] Reported values of λ_1^a and f are the optimal solution that minimizes the squared error between the observed and the theoretical zeroth and first temporal moments for Raz. The observed moments are calculated from data with equation (14) and the theoretical moments are calculated with equations (19) and (20). The minimized squared error was calculated using Excel's Solver with the constraints: $0 \leq f \leq 1$ and $\lambda_1^a \geq 0$.

4. Results

4.1. Physical and Biological Characterization of the Reaches

[25] Discharge was 1.25 L s^{-1} at the bottom of the bedrock reach and increased to 1.34 L s^{-1} at the bottom of the

Table 1. Physical Characteristics and Ecosystem Respiration Rates of the Two Reaches

	Bedrock Reach (S0-S12)	Alluvial Reach (S12-S20)
Reach length (m)	357.5	205.7
Slope (m m^{-1})	0.16	0.14
Discharge (L s^{-1})	1.25	1.34
Water velocity (cm s^{-1})	3.68	1.35
Average wetted width (m)	1.91	2.04
Average depth (cm)	1.78	4.85
Temperature ($^{\circ}\text{C}$) ^a	12.0 \pm 0.0	11.9 \pm 0.1
DO saturation (%) ^a	94.54 \pm 0.01	92.34 \pm 0.02
Ecosystem respiration ($\text{g O}_2 \text{ m}^{-2} \text{ d}^{-1}$) ^b	0.24 \pm 0.00	0.44 \pm 0.00

^aAverage \pm SE. Temperature, DO saturation, and ecosystem respiration were measured during 6 h at night beginning at sunset. Average ecosystem respiration rate from this period was extrapolated to 24 h to estimate a daily rate.

^bSE of ER calculated based on the uncertainty of k (i.e., calculating ER using maximum and minimum k estimates).

alluvial reach, mainly due to the inflow from the small tributary. The bedrock reach had a narrower and shallower wetted channel with $2.7 \times$ faster water velocity than the alluvial reach (Table 1). Although the bedrock reach was $1.7 \times$ longer than the alluvial reach, the nominal travel time was only $0.6 \times$ that of the alluvial reach, and the mean travel time was $0.23 \times$ that of the alluvial reach (Table 2).

[26] Average water temperature during night was similar in both reaches and averaged ca. 12°C (Table 1). During this period, DO saturation was relatively high in both reaches, but was 2.2% higher in the bedrock reach than in the alluvial reach (Table 1; Wilcoxon test, $Z = -7.57$, $d.f. = 76$, $p < 0.001$).

[27] Whole-reach daily ER was $1.8 \times$ higher in the alluvial reach than in the bedrock reach (Table 1). Regression methods for estimating k gave significant slopes and intercepts ($p < 0.001$) and very low k values with low standard errors ($-0.0085 \pm 0.0009 \text{ h}^{-1}$ in the bedrock reach and

Table 2. Hydraulic Parameters, Transport of Resazurin (Raz), and Size of the MATS of the Two Reaches^a

	Bedrock Reach (S0-S12)	Alluvial Reach (S12-S20)
Relative size of transient storage zone (A_s/A , -) ^b	0.19	2.45
Nominal travel time (t_n , h)	2.7	4.2
Mean travel time of EC (τ , h)	3.5	15.3
Dal	5.4	1.4
F_{med} (%)	9.5	44.1
Raz uptake length (S_{w-Raz} , m)	1085	140
Raz uptake velocity (V_{f-Raz} , mm min^{-1})	0.036	0.281
MATS fraction in transient storage zone (f , -)	0.37	1.00
Size of the MATS zone (m^2)	0.002	0.291
Effective reaction rate coefficient of MATS zone (λ_e^a , h^{-1})	1.88	0.12
Volume-weighted effective reaction rate coefficient of MATS zone ($\beta f \lambda_e^a$, h^{-1})	0.13	0.29

^aEC, electrical conductivity.

^bEstimated using OTIS-P.

$0.0136 \pm 0.0023 \text{ h}^{-1}$ in the alluvial reach). In the bedrock reach, instantaneous respiration was stable during the measurement period fluctuating between 0.23 and $0.26 \text{ g O}_2 \text{ m}^{-2} \text{ d}^{-1}$. In the alluvial reach instantaneous respiration was relatively constant until 2 h after the sunset, fluctuating between 0.39 and $0.44 \text{ g O}_2 \text{ m}^{-2} \text{ d}^{-1}$, and then gradually increased, reaching its maximum ($0.50 \text{ g O}_2 \text{ m}^{-2} \text{ d}^{-1}$) by the end of the measurement period.

4.2. Surface Results of Solute Tracers

4.2.1. Analysis of the Breakthrough Curves

[28] The shapes of the EC profiles over time indicate clear differences between the hydraulic characteristics of the two reaches. The bedrock reach showed a BTC for EC typical of a reach with moderate A_s/A , with a sharp rise, a shoulder on the rising limb, a sharp decline, and a low-concentration tail (Figure 3a). In contrast, the alluvial reach showed a BTC for EC typical of a reach with large A_s/A , with a slow rise and a slow fall with an extended tail (Figure 3b). A_s/A , estimated by OTIS-P, was 0.19 in the bedrock reach and it contributed 9.5% to the median water travel time (F_{med}^{200} , Table 2). A_s/A was 2.45 in the alluvial reach and it contributed 44.1% to the median water travel time (Table 2). Dal values measured 5.4 in the bedrock reach and 1.4 in the alluvial reach (Table 2). Although ideal values of Dal should be ~ 1.0 to ensure maximum reliability of estimated hydraulic parameters, values observed in our reaches are within reasonable bounds. The bedrock reach arrived at plateau 6.5 h after the injection began and recovered to pre-addition values 23 h

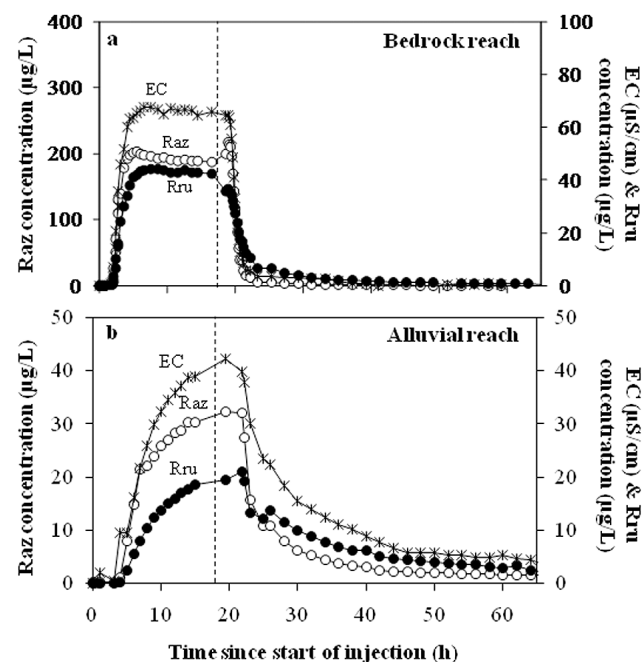


Figure 3. Break-through curves for background-corrected electrical conductivity (EC, asterisks), resazurin concentration (Raz, open circles), and resorufin concentration (Rru, closed circles) measured at the end (a) of the bedrock reach and (b) of the alluvial reach. Note the difference in the range of values between Raz and Rru concentrations when comparing Raz and Rru within each reach. Vertical dashed lines show the time when injection was stopped.

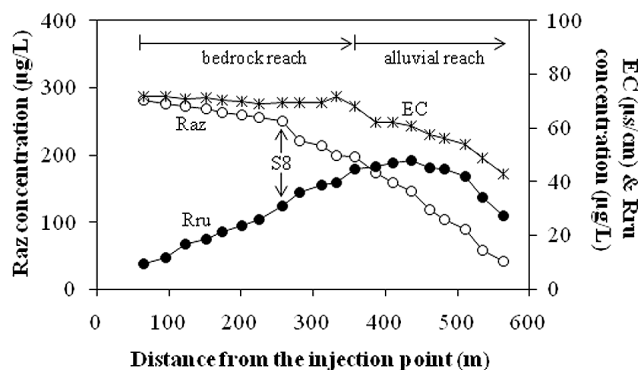


Figure 4. Variation of background-corrected electrical conductivity (EC, asterisks), resazurin concentration (Raz, open circles), and resorufin concentration (Rru, closed circles) in surface water along the two reaches. Raz and Rru concentrations have been multiplied by the dilution factor (i.e., by EC at the injection site/EC at the sampling site). Samples were collected before the injection was stopped (i.e., after 17 h of solute injection). The arrow highlights a change/break in Raz and Rru longitudinal profile near the end of the bedrock reach (station S8).

after the injection was stopped. The alluvial reach did not arrive at plateau during the injection and did not recover to pre-injection values by the end of the measurements (49 h after the injection was stopped).

[29] In the bedrock reach, Raz was higher than Rru (Figure 3a). During plateau, Raz and Rru slightly decreased over time. This decrease was not explained by variation in the solute injection rate because it was not observed for EC. Additionally, Raz concentration showed a sharp increase and Rru concentration showed a decrease 2 h after the stop of the injection. By the end of the experiment we only recovered 90% of the sum of Raz and Rru injected. In the alluvial reach, Raz was also higher than Rru (Figure 3b) but the difference between Raz and Rru concentrations was smaller than in the bedrock reach. Raz and Rru concentrations gradually increased until 2 h after the end of the injection and then gradually decreased. We only recovered 37.2% of the mass of Raz and Rru that entered the alluvial reach.

4.2.2. Longitudinal Profile

[30] The transformation of Raz to Rru was heterogeneous along the bedrock reach. While the longitudinal EC profile was relatively steady, Raz concentration decreased uniformly until S8, where a sharper decline was observed (Figure 4). In contrast, Rru concentration gradually increased along the bedrock reach. Along the alluvial reach, EC decreased with distance because we did not achieve plateau conditions at the most downstream points. As in the bedrock reach, Raz concentration gradually decreased along the reach. However, Rru concentration increased with distance in the first 3 sampling sites (i.e., from S13 to S15) and then gradually decreased towards the downstream end of the reach (Figure 4).

4.2.3. Transport and Transformation of Raz

[31] The uptake length for Raz was 7.8 times longer in the bedrock reach than in the alluvial reach (Table 2). The uptake velocity (V_{f-Raz}) was 0.13 as fast in the bedrock reach

as in the alluvial reach. The fraction of MATS was 0.37 in the bedrock reach but was 1.0 in the alluvial reach. In the alluvial reach, we measured whole-reach ecosystem respiration simultaneously with the injection; and thus, we were able to examine the relationship between the Rru:Raz molar ratio and the instantaneous respiration rates which were positively related ($r^2 = 0.76$, $n = 7$, $p = 0.01$, Figure 5).

[32] While the whole-stream measurements indicated that the bedrock reach was much slower at transforming Raz, the reaction rate coefficient within the MATS in the bedrock reach was high. The effective reaction rate coefficient λ_e^a for Raz was $16 \times$ larger in the bedrock reach than in the alluvial reach. At the same time, the volume-weighted effective reaction rate coefficient for Raz was $2.2 \times$ larger in the alluvial reach than in the bedrock reach, a factor which is similar in magnitude to the difference in respiration ($1.8 \times$). We emphasize these results and will discuss them further below.

4.3. Hyporheic Results

[33] Data from wells indicated higher transformation of Raz in the hyporheic zone than in the surface channel of the alluvial reach although we observed large variability in EC, Raz, and Rru concentrations between individual wells. All wells except W5 and W11 showed an increase in EC within 26 h after the solute injection started, but only 3 of them reached a clear plateau before the end of the injection. The first arrival time ranged between 2.8 and 13.5 h among wells, and the degree of connection with surface water ranged between 10.6 and 65.5% (Table 3). Raz and Rru concentrations varied among wells ranging between 0.00 and $26.39 \mu\text{g Raz/L}$ and 0.00 and $17.49 \mu\text{g Rru/L}$. Raz and Rru concentrations at wells (corrected by the percentage of surface water present in the wells) were lower than at the adjacent surface sampling point indicating a loss of both solutes in the hyporheic zone (Table 3). We further explore if these differences were due to higher transformation in hyporheic zone or were caused by hydrological factors. We compared the transformation of Raz to Rru in the hyporheic zone relative to that in the surface zone. Well 7 was

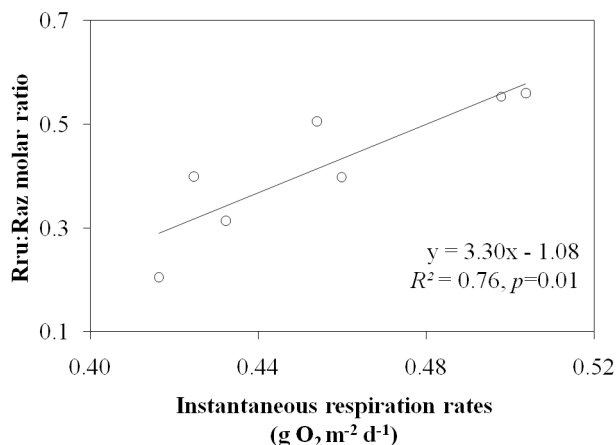


Figure 5. Relationship between instantaneous respiration rates and the resorufin:resazurin ratio estimated from the break-through curves data. Data are from the alluvial reach where the two measurements were done simultaneously.

Table 3. Transport and Surface Water Exchange Characteristics for Each of the Wells^a

Well	First Arrival Time (h)	% SW	[Raz] ($\mu\text{g L}^{-1}$)	[Rru] ($\mu\text{g L}^{-1}$)
W1	13.5	60.5	9.92	7.23
W2	4.9	63.9	15.21	11.07
W3	7.1	65.5	26.39	17.49
W4	6.9	10.6	1.61	0.92
W6	5.0	14.1	0.25	0.18
W7	6.8	15.2	0.00	0.00
W8	2.8	48.9	4.64	3.68
W9	12.3	53.7	19.36	13.50
W10	12.2	30.3	1.33	0.99
S20	2.0	100	32.26	19.90

^aWells (W) were located near surface station S20 (Figure 1). Raz and Rru are the peak concentrations scaled by %SW. For comparison, data from surface sampling station S20 are also included. Data from wells W5 and W11 are not shown because these wells did not show breakthrough.

excluded from the analysis since we did not observe Raz nor Rru. On average, corrected Rru:Raz molar ratios were significantly higher in the hyporheic zone than at surface (Wilcoxon test, $Z = -2.38$, $p = 0.02$, $n = 8$; Figure 6).

5. Discussion

5.1. WS03 Dynamics and Metabolism

[34] The reaches differed in terms of both hydraulic parameters and metabolic activity. The relative size of the transient storage zone was 12.7 times larger and the mean water residence time was 4.3 longer in the alluvial reach than in the bedrock reach. The relative sizes of the transient storage zones agree with other previous studies conducted in these reaches [Gooseff *et al.*, 2005; Wondzell, 2006]. The value of A_s/A measured in the bedrock reach by Gooseff *et al.* (0.14) was in the same range as the present study; however, their A_s/A measured in the alluvial reach (105) was much larger than the 2.45 from this study. Most of this difference was probably due to the different tracers used in the two studies. While Cl is conservative, rhodamine WT used in the previous [Gooseff *et al.*, 2005] work can sorb to sediments [Bencala *et al.*, 1983], therefore in our opinion, the value measured by Cl in this study is probably more accurate.

[35] Metabolic activity measured by changes in DO, was higher in the alluvial than in the bedrock reach. Despite differences between reaches, daily rates of ecosystem respiration were in the range of other streams of similar size from the same region. For instance, Bott *et al.* [1985] measured ecosystem respiration seasonally at 4 reaches of increasing size at the H.J. Andrews Experimental Forest and the obtained values were $0.36 \pm 0.19 \text{ g O}_2 \text{ m}^{-2} \text{ d}^{-1}$ in a first-order stream and $0.42 \pm 0.22 \text{ g O}_2 \text{ m}^{-2} \text{ d}^{-1}$ in a second-order stream. Naiman and Sedell [1980] also found respiration values ranging between 0.2 and $0.7 \text{ g O}_2 \text{ m}^{-2} \text{ d}^{-1}$ in streams from or close to the H.J. Andrews Experimental Forest. However, both studies used chambers to estimate benthic respiration, so they do not truly reflect ER because chambers do not completely integrate hyporheic respiration. In general, ER in this region is in the lower range of reported values for streams worldwide [Mulholland *et al.*, 2001; Acuña *et al.*, 2004; Ortiz-Zayas *et al.*, 2005].

[36] Differences in ecosystem respiration between the two study reaches were consistent with what we expected from

the literature based on differences in transient storage size. Several authors have shown a positive relationship between size of transient storage zones and respiration. For instance, Fellows *et al.* [2001] showed that reaches from the same stream that had larger A_s/A also had higher ER. Mulholland *et al.* [1997] found that metabolism and nutrient uptake rates were substantially higher in a stream with a large transient storage zone than in a similar stream with a small transient storage zone. In an inter-biome study encompassing 8 relatively pristine streams, Mulholland *et al.* [2001] concluded that ER was significantly correlated with inorganic phosphorus concentration and size of the transient storage zone and, together, these factors explained 73% of the variation in ER. In contrast, Bernot *et al.* [2010] found that transient storage did not relate to metabolism in a study done in 70 streams however their study included streams with diverse land-uses and thus probably with human-altered A_s/A .

5.2. Resazurin as a Metabolic Tracer

[37] The use of Raz as a metabolic tracer is supported by (1) the difference in the whole-reach Raz processing efficiency (expressed as the uptake length and uptake velocity of Raz, and as the volume-weighted effective Raz reaction rate coefficient) observed between reaches; and (2) the positive relationship observed between Rru:Raz molar ratios and instantaneous respiration rates. This relationship was also observed in a lab and field study by Haggerty *et al.* [2008, 2009] in which they injected Raz and measured ecosystem respiration in a Mediterranean headwater stream. In that case, the reach had higher ecosystem respiration ($1.30 \text{ g O}_2 \text{ m}^{-2} \text{ d}^{-1}$) and higher Raz processing efficiency (i.e., shorter Raz uptake length, S_{w-Raz} 674 m; and faster uptake velocity, $V_{f-Raz} = 0.69 \text{ mm min}^{-1}$) than what we observed in WS03.

[38] The use of Raz also allowed us to observe spatial heterogeneity in metabolic activity through the analysis of the longitudinal profiles i.e., through changes in the ratios of Rru to Raz along the reach. Unfortunately, because plateau conditions were not achieved in the alluvial reach, we could only examine these changes in the bedrock reach. The longitudinal profile of Rru to Raz ratios in the bedrock reach showed a sharp increase over the last 133 m, which corre-

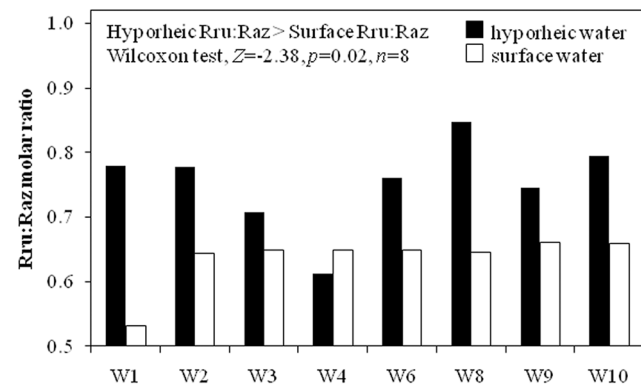


Figure 6. Rru:Raz molar ratio in hyporheic water (black bars) in comparison to surface channel water (white bars) after correcting by percentage of surface water present in wells.

sponded to a segment that, although scoured to bedrock, presented some alluvial deposits and some vegetation on the banks. Thus, this downstream portion of the bedrock reach was susceptible to contain more MATS than the upstream segment. Additionally, the great variability in Rru:Raz molar ratios observed at wells indicated heterogeneity in metabolic activity among flowpaths in the hyporheic zone.

[39] The longitudinal changes seen in the bedrock reach suggest that Raz is sensitive to changes in metabolic activity at a whole-reach scale but also at smaller scales such as morphological units, and opens new perspectives and possibilities in the study of ecosystem metabolism. Our results support the idea of using Raz as a metabolic tracer to infer rates of ecosystem respiration *in situ* without the need to estimate reaeration rates, which is proved to be a critical source of error in metabolism measurements [McCutchan *et al.*, 1998], and without the need to use incubation chambers which are known to be not spatially representative of ecosystem metabolism under natural conditions [Grimm and Fisher, 1984; Bott, 2006]. Since the Raz to Rru reaction is irreversible, and since this reaction only happens in the presence of living organisms [McNicholl *et al.*, 2007], this transformation could, in the future, be used as a measure of the consumption of DO in the reach.

5.3. Parameter Estimation Methods

[40] The method of temporal moments used to calculate the model parameters is encouraging since it is easy to apply and it provided estimates of the Raz uptake length and the size of the MATS that were consistent with what we observed from the comparison of Raz and Rru concentrations at wells and in the adjacent surface zone. Additionally, the method of temporal moments allows the estimation of metabolic parameters without the need to arrive at plateau conditions. This can be convenient in streams with high discharge where an injection to plateau conditions would require a huge amount of tracer to inject. However, the parameters estimated by the method of temporal moments are subjected to uncertainty.

[41] Part of the uncertainty involved in the estimation of Raz parameters (i.e., f , λ_1^a) depends on the uncertainty linked to the estimation of hydraulic parameters (i.e., α , A_s , and A). We used the standard deviations of those parameters reported in OTIS-P to estimate f and λ_1^a under two different scenarios: maximum and minimum values of hydraulic parameters. The f in the bedrock reach was 0.42 with maximum hydraulic parameters and 0.32 with minimum hydraulic parameters. The f in the alluvial reach, and values of λ_1^a in both reaches, did not change with hydraulic parameters.

[42] Another source of uncertainty is linked to the observed loss of the tracer which will discuss in more detail in the following section. Finally, other sources of uncertainty and limitations of the technique are those inherent to all tracer techniques (i.e., tracer results only detect a small window of the total water exchange flowpaths present in the reach although it detects the flowpaths with higher probability to impact metabolism at a whole-reach scale) [Harvey and Wagner, 2000].

5.4. Dye Loss and Effects on Parameter Estimation

[43] Some open questions remain about the loss of mass at the end of the reaches (8.4% at the end of the bedrock reach

and 62.8% at the end of the alluvial reach) and the effect on estimated parameters. Mass loss was also observed by Haggerty *et al.* [2009]. There is evidence of Rru photodegradation in laboratory experiments [Haggerty *et al.*, 2008], and thus, some of the observed loss could be explained by the exposure of the compound to sunlight during the study. In addition, we hypothesize that a fraction of the mass loss could be attributable to (1) a transformation of both Raz and Rru to unknown compounds (accounted for in the model), (2) an inaccurate discharge measurement, and (3) to sorption to sediments and organic matter, some of which is probably irreversible on the timescale of the experiment.

[44] The amount of dye loss has some uncertainty due to uncertainties in the discharge. We assumed that the only process affecting the water balance is a gain of water along the reach but more realistic is that the reaches are gaining and losing water, and thus, gaining chloride and losing dye and chloride. If the EC of the gained water is higher than surface background conditions, we would overestimate the loss of the dye. Ideally, we should have independent measures of discharge [Payn *et al.*, 2009] that would allow us to measure the mass recovery of the conservative tracer. Wondzell [2006], in the same wells as those used in this study, observed a higher increase in EC in the wells than in the surface water at the end of the reach which Payn *et al.* [2009] related to a loss in the mass recovered. However, we did not observe a higher increase in EC in the wells than in the surface water. Therefore, although it is possible, we cannot conclude that the reaches suffered a loss of water.

[45] Finally, Raz and Rru are subjected to sorption to the sediment. Haggerty *et al.* [2008] reported a distribution coefficient, K_d , of 6.63 mL g⁻¹ for Rru (they could not measure the sorption isotherm for Raz because the compound reduces to Rru in the presence of aerobic bacteria in sediment and, in any case, sorption of Raz and Rru should be very similar because of their nearly identical chemical structure). Laboratory experiments using different sediments (data not reported) indicate a positive relation between the amount of dye loss and the organic matter content of the sediment. The effects of sorption should be reflected either in λ_1^a (if sorption is affecting Raz) and/or in λ_2^a (if sorption is affecting Rru). Since transformation rate coefficients measured in previous experiments are relatively fast and microbial biomass and activity are higher in sediments with high organic matter content [Fischer *et al.*, 1996], we expect some Raz to transform to Rru before being sorbed, and thus that sorption affects mainly the Rru form. In this case, because the estimation of f and λ_1^a only uses Raz temporal moments, the estimation of the parameters would not be affected by sorption.

[46] To calculate the effects of sorption of Raz on the estimates of f and λ_1^a we included a irreversible sorption rate coefficient λ_1^s (h⁻¹) in the Raz transport and temporal moment equations. Basically, we replaced every λ_1^a and λ_1^i by the sum of two rate coefficients, one due to biological processes and the other due to irreversible sorption ($\lambda_1^{a,bio} + \lambda_1^{a,s}$, and $\lambda_1^{i,bio} + \lambda_1^{i,s}$). We assumed negligible sorption of Raz in the water column and identical sorption of Raz in the MATS and the MITS zones. We then estimated f and $\lambda_1^{a,bio}$, and calculated λ_e^a for a reasonable range of sorption rates based on what is known for rhodamine WT [Sutton *et al.*, 2001].

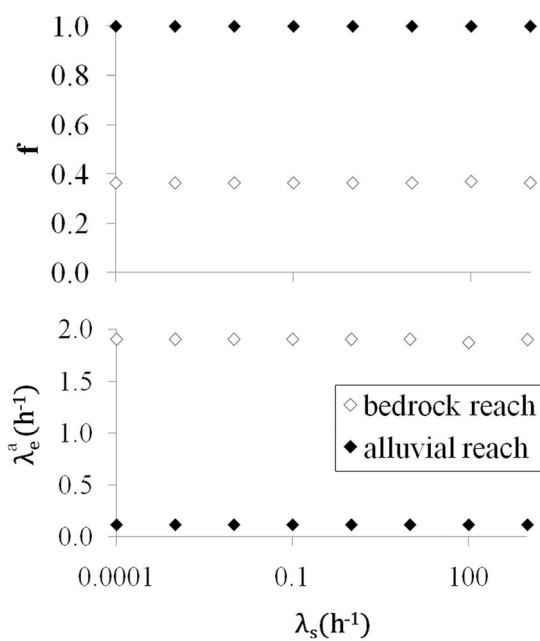


Figure 7. Effects of varying the sorption rate coefficient of Raz on the estimated values of f and λ_e^a , in the bedrock reach (white symbols) and in the alluvial reach (black symbols).

Results of those simulations (Figure 7) indicate that f and λ_e^a estimates are robust to irreversible sorption. In other words, the loss of tracer potentially due to irreversible sorption probably did not affect our estimates of the effective reaction rate coefficient or the fraction of MATS.

5.5. Surface Versus Hyporheic MATS

[47] Metabolic activity, measured both by changes in DO and Raz transformation, was higher in the alluvial reach than in the bedrock reach. While our metabolism results agree with previous findings (i.e., higher respiration in the reach with larger transient storage), the use of Raz and the concept of MATS allow us to further understand important differences between a reach dominated by surface transient storage (the bedrock reach) and a reach dominated by hyporheic transient storage (the alluvial reach).

[48] While the transient storage size was ca. 13 times higher in the alluvial reach, ecosystem respiration was only 2 times higher. This suggests a differential metabolic contribution of the transient storage zones in the two reaches, with the MATS in the alluvial reach proportionally less active than that in the bedrock reach. In fact, reaction rates within MATS (the effective reaction rate coefficient, λ_e^a) were ca. 16 times faster in the bedrock reach (surface MATS) than in the alluvial reach (hyporheic MATS). This observation indicates that while whole-stream respiration is lower in the bedrock reach than in the alluvial reach, the MATS in the bedrock reach has higher rates of metabolism. However, the higher rate coefficient in the bedrock MATS was offset by the MATS measuring only 0.002 m^2 in the bedrock reach in comparison to 0.291 m^2 in the alluvial reach.

[49] The effective reaction rate coefficient for Raz (λ_e^a) in the bedrock reach was 1.9 h^{-1} , a result similar to the bio-

logical reaction rate coefficient (λ_1^a) for Raz of 1.55 h^{-1} measured in colonized hyporheic sediments by *Haggerty et al.* [2008]. However, the effective reaction rate coefficient in the alluvial reach was only 0.12 h^{-1} . The reason for the difference can be explained by examining equation (21b). The effective reaction rate coefficients result from the interaction between hydrology (i.e., α_2 , the water exchange rate coefficient between free-flowing water and transient storage zones) and biology (i.e., biological reaction rate coefficients at MATS; λ_1^a). The bedrock reach exhibits a rapid exchange between the channel and the transient storage ($\alpha_2 = 1.69 \text{ h}^{-1}$). However, to obtain an effective rate coefficient of 1.9 h^{-1} , the biological reaction rate coefficient must also be fast ($>1.9 \text{ h}^{-1}$), a conjecture supported by the data of *Haggerty et al.* [2008] as well as similar rate coefficients we have collected for other Oregon streams. Therefore, we conclude that in the bedrock reach, both hydrology and biology control the whole-stream metabolic activity. In contrast, in the alluvial reach, the exchange rate coefficient between the channel and hyporheic transient storage is much slower ($\alpha_2 = 0.09 \text{ h}^{-1}$). The effective reaction rate coefficient (λ_e^a) is 0.12 h^{-1} . It is reasonable to assume that the biological reaction rate coefficient of Raz is $>1 \text{ h}^{-1}$, as we have seen in other studies. Therefore, we conclude that hydrologic exchange (specifically, the advection rate into the hyporheic zone) regulates metabolic activity in the hyporheic zone, which in turn may contribute to whole reach metabolic patterns observed in surface water, as similarly reported in other studies [e.g., *Harvey and Fuller*, 1998; *Fellows et al.*, 2001; *Fuller and Harvey*, 2000]. In summary, in WS03, metabolism associated with surface MATS is controlled both by hydrology and biology while metabolism in hyporheic MATS is limited by the supply of oxygen and reactive solutes that fuel aerobic biological activity in this compartment (Figure 2). In turn, hydrological exchange may also determine the extent in which hyporheic metabolic activity manifests at surface water as suggested by *Findlay* [1995].

[50] *Findlay* [1995] proposed a conceptual model in which the functional significance of the hyporheic zone from a stream ecosystem perspective was determined by surface-subsurface hydrological exchange and rates of hyporheic biogeochemical processes. Results from *Battin* [1999, 2000] present hydrodynamics as a template that drives microbial and biogeochemical processes on the sediment and reach scales. Our results support these conceptual models and give insight into previously contradictory results in studies comparing metabolic activity in surface and hyporheic transient storage zones. For example, *Romani et al.* [1998], and *Gücker and Boëchat* [2004] found higher metabolic activity in the surface benthic zone than in the hyporheic zone, while *Grimm and Fisher* [1984] and *Mulholland et al.* [1997] found that hyporheic transient storage was more important for metabolism and nutrient cycling. It is clear that under different conditions either surface or hyporheic transient storage can have greater metabolic activity. For example, we would hypothesize that most of the metabolism would be located in surface transient storage in a stream with large quantity of shallow surface transient storage and rapid exchange. However, hyporheic transient storage would host most of the metabolism in a stream with large quantity of rapid hyporheic exchange and without much

surface transient storage (or surface transient storage that has very slow exchange or deep pools).

6. Conclusions

[51] Resazurin can be used as a sensitive tracer to quantify metabolically active transient storage (MATS). Rru to Raz ratios are shown here to be a function of respiration rates. In addition, Raz is shown to be sensitive to differences in channel configuration and morphology at the reach scale as well as to spatial heterogeneity in habitat within the reach. Therefore, Raz as a “smart” tracer can overcome some of the limitations of conventional respiration measurement methods. For example, the method of using incubation chambers leads to difficulties in upscaling results to a whole-reach level. While the upstream-downstream dissolved oxygen change technique measures respiration at whole-reach level but does not provide information about spatial heterogeneity in metabolic rates. Since Raz to Rru conversion is an irreversible process which occurs in the presence of microbial metabolism, the Raz method could be developed to measure “in situ” stream respiration. Further, Raz provides previously unavailable information on the efficiency of stream reaches in transforming solutes via metabolic activity, and on the separation of that metabolic activity between different stream compartments.

[52] In summary, the methodology presented in this paper allowed us to make comparisons of metabolism patterns in WS03 simultaneously at a reach and at a smaller scale. Further, the Raz tracer method is affordable (Raz used in this experiment cost less than USD \$200) and relatively easy to apply (it only requires the use of a spectrofluorometer to analyze the samples). Last, the simultaneous injection of a conservative tracer and Raz allows us to quantify MATS and to advance the understanding of the role that transient storage zones play on stream metabolic processes at a whole-reach scale.

Notation

A stream cross-sectional area, m^2 .
 A_s cross-sectional area of sum of storage zones, m^2 .
 C concentration in stream, $\mu g L^{-1}$.
 D dispersion coefficient, $m h^{-2}$.
 Def average DO saturation deficit in the reach, $mg O_2 L^{-1}$.
 DO_{down} DO concentration downstream, $mg O_2 L^{-1}$.
 DO_{up} DO concentration upstream, $mg O_2 L^{-1}$.
 f fraction of storage zone volume that is metabolically active.
 L reach length, m.
 h water depth, m.
 M_{Raz} molecular weight of Raz = 251.2 $g mol^{-1}$, $g mol^{-1}$.
 k_2 reaeration rate coefficient adjusted to streamwater temperature, h^{-1} .
 M_{Rru} molecular weight of Rru = 235.2 $g mol^{-1}$, $g mol^{-1}$.
 $m_{0,EC}^d$ zeroth moment at the downstream location for EC, $\mu S cm^{-1} h$.
 $m_{0,Raz}^d$ zeroth moment at the downstream location for Raz, $\mu g L^{-1} h$.
 $m_{1,EC}^d$ first moment at the downstream location for EC, $\mu S cm^{-1} h^2$.

$m_{1,Raz}^d$ first moment at the downstream location for Raz, $\mu g L^{-1} h^2$.
 $m_{0,EC}^u$ zeroth moment at the upstream location for EC, $\mu S cm^{-1} h$.
 $m_{0,Raz}^u$ zeroth moment at the upstream location for Raz, $\mu g L^{-1} h$.
 $m_{1,EC}^u$ first moment at the upstream location for EC, $\mu S cm^{-1} h^2$.
 $m_{1,Raz}^u$ first moment at the upstream location for Raz, $\mu g L^{-1} h^2$.
 Q stream discharge, $m^3 h^{-1}$.
 S^a solute concentration in metabolically active storage zone, $\mu g L^{-1}$.
 S^i solute concentration in metabolically inactive storage zone, $\mu g L^{-1}$.
 S_{w-Raz} Raz uptake length, m.
 t time, h.
 t_n nominal travel time between the upstream and the downstream sampling point for free flowing water in main channel, h.
 u water velocity, $m h^{-1}$.
 V_{f-Raz} Raz uptake velocity, $mm min^{-1}$.
 w average wetted width of the reach, m.
 x longitudinal coordinate, m.
 y^a conversion factor, $y^a = \lambda_{12}^a \frac{M_{Rru}}{M_{Raz}}$.
 y^i conversion factor, $y^i = \lambda_{12}^i \frac{M_{Rru}}{M_{Raz}}$.
 α exchange rate coefficient in the transient storage zone, h^{-1} .
 α_2 $\alpha_2 = \alpha A/A_s$, h^{-1} .
 β (A_s/A).
 τ mean travel time between the upstream and the downstream sampling point including time in the transient storage zone, h.
 λ_e^a effective reaction rate coefficient for MATS, h^{-1} .
 λ_1^a sum of Raz to Rru transformation rate coefficient and Raz decay rate coefficient in MATS, h^{-1} .
 $\lambda_1^{a,bio}$ part of λ_1^a due to biological processes, h^{-1} .
 $\lambda_1^{a,s}$ part of λ_1^a due to irreversible sorption, h^{-1} .
 λ_{12}^a Raz to Rru transformation rate coefficient in MATS, h^{-1} .
 λ_2^a Rru decay rate coefficient in MATS, h^{-1} .
 λ_1^i sum of Raz to Rru transformation rate coefficient and Raz decay rate coefficient in MITS (obtained experimentally from Haggerty *et al.* [2008], equivalent to $k_1 + k_{12} = 2.89 \times 10^{-7} + 9.89 \times 10^{-4} h^{-1}$), h^{-1} .
 $\lambda_1^{i,bio}$ part of λ_1^i due to biological processes, h^{-1} .
 $\lambda_1^{i,s}$ part of λ_1^i due to irreversible sorption, h^{-1} .
 λ_1^s irreversible sorption rate coefficient, h^{-1} .
 λ_{12}^i Raz to Rru transformation rate coefficient in MITS (obtained experimentally from Haggerty *et al.* [2008], equivalent to $k_{12} = 9.89 \times 10^{-4} h^{-1}$), h^{-1} .
 λ_2^i Rru decay rate coefficient in MITS (obtained experimentally from Haggerty *et al.* [2008], equivalent to $k_2 = 1.75 \times 10^{-3} h^{-1}$), h^{-1} .

[53] **Acknowledgments.** We thank Sherri Jonhson, Linda Ashkenas, Steve Wondzell for equipment and advice, Julia Jones, and the OSU GEO 548 field research class for help during the experiment. Data and facilities were provided by the H.J. Andrews Experimental Forest research program, funded by the National Science Foundation’s Long-Term Ecological Research Program (DEB 08-23380), US Forest Service Pacific Northwest Research Station, and Oregon State University. Financial support was provided by the Catalan Government through a BE grant (2007-BE100157),

and by the National Science Foundation (EAR 04-09534 and EAR 08-38338).

References

- Acuña, V., A. Giorgi, I. Muñoz, U. Uehlinger, and S. Sabater (2004), Flow extremes and benthic organic matter shape the metabolism of a headwater Mediterranean stream, *Freshwater Biol.*, 49(7), 960–971, doi:10.1111/j.1365-2427.2004.01239.x.
- Argerich, A., E. Marti, F. Sabater, M. Ribot, D. von Schiller, and J. Riera (2008), Combined effects of leaf litter inputs and a flood on nutrient retention in a Mediterranean mountain stream during fall, *Limnol. Oceanogr.*, 53(2), 631–641, doi:10.4319/lo.2008.53.2.0631.
- Aris, R. (1958), On the dispersion of linear kinematic waves, *Proc. R. Soc. London, Ser. A*, 245, 268–277, doi:10.1098/rspa.1958.0082.
- Battin, T. J. (1999), Hydrologic flow paths control dissolved organic carbon fluxes and metabolism in an alpine stream hyporheic zone, *Water Resour. Res.*, 35(10), 3159–3169, doi:10.1029/1999WR900144.
- Battin, T. J. (2000), Hydrodynamics is a major determinant of streambed biofilm activity: From the sediment to the reach scale, *Limnol. Oceanogr.*, 45(6), 1308–1319, doi:10.4319/lo.2000.45.6.1308.
- Bencala, K. E., and R. A. Walters (1983), Simulation of solute transport in a mountain pool-and-riffle stream: A transient storage model, *Water Resour. Res.*, 19(3), 718–724, doi:10.1029/WR019i003p00718.
- Bencala, K. E., R. E. Rathbun, A. P. Jackman, V. C. Kennedy, G. W. Zellweger, and R. J. Avanzino (1983), Rhodamine WT dye losses in a mountain stream environment, *J. Am. Water Resour. Assoc.*, 19(6), 943–950.
- Bernot, M. J., et al. (2010), Inter-regional comparison of land-use effects on stream metabolism, *Freshwater Biol.*, 55, 1874–1890, doi:10.1111/j.1365-2427.2010.02422.x.
- Bott, T. L. (2006), Primary productivity and community respiration, in *Methods in Stream Ecology*, 2nd ed., edited by F. R. Hauer and G. A. Lamberti, pp. 663–690, Academic, San Diego, Calif.
- Bott, T. L., J. T. Brock, C. S. Dunn, R. J. Naiman, R. W. Ovink, and R. C. Petersen (1985), Benthic community metabolism in four temperate stream systems: an inter-biome comparison and evaluation of the river continuum concept, *Hydrobiologia*, 123(1), 3–45, doi:10.1007/BF00006613.
- Briggs, M. A., M. N. Gooseff, C. D. Arp, and M. A. Baker (2009), A method for estimating surface transient storage parameters for streams with concurrent hyporheic storage, *Water Resour. Res.*, 45, W00D27, doi:10.1029/2008WR006959.
- Bukaveckas, P. A. (2007), Effects of channel restoration on water velocity, transient storage, and nutrient uptake in a channelized stream, *Environ. Sci. Technol.*, 41(5), 1570–1576, doi:10.1021/es061618x.
- Butturini, A., and F. Sabater (1999), Importance of transient storage zones for ammonium and phosphate retention in a sandy-bottom Mediterranean stream, *Freshwater Biol.*, 41(3), 593–603, doi:10.1046/j.1365-2427.1999.00406.x.
- Elmore, H. L., and W. F. West (1961), Effect of water temperature on stream re-aeration, *J. Sanit. Eng. Div.*, 87(SA6), 59–71.
- Ensign, S. H., and M. W. Doyle (2005), In-channel transient storage and associated nutrient retention: Evidence from experimental manipulations, *Limnol. Oceanogr.*, 50(6), 1740–1751, doi:10.4319/lo.2005.50.6.1740.
- Fellows, C. S., H. M. Valett, and C. Dahm (2001), Whole-stream metabolism in two montane streams: Contribution of the hyporheic zone, *Limnol. Oceanogr.*, 46(3), 523–531, doi:10.4319/lo.2001.46.3.0523.
- Fellows, C. S., H. M. Valett, C. N. Dahm, P. J. Mulholland, and S. A. Thomas (2006), Coupling nutrient uptake and energy flow in headwater streams, *Ecosystems*, 9(5), 788–804, doi:10.1007/s10021-006-0005-5.
- Findlay, S. (1995), Importance of surface-subsurface exchange in stream ecosystems: the hyporheic zone, *Limnol. Oceanogr.*, 40(1), 159–164, doi:10.4319/lo.1995.40.1.0159.
- Fischer, H., M. Pusch, and J. Schwoerbel (1996), Spatial distribution and respiration of bacteria in stream-bed sediments, *Arch. Hydrobiol.*, 137(3), 281–300.
- Fuller, C. C., and J. W. Harvey (2000), Reactive uptake of trace metals in the hyporheic zone of a mining-contaminated stream, Pinal Creek, Arizona, *Environ. Sci. Technol.*, 34(7), 1150–1155, doi:10.1021/es990714d.
- Goltz, M. N., and P. V. Roberts (1987), Using the method of moments to analyze three-dimensional diffusion-limited solute transport from temporal and spatial perspectives, *Water Resour. Res.*, 23(8), 1575–1585, doi:10.1029/WR023i008p01575.
- Gooseff, M. N., D. M. McKnight, R. L. Runkel, and J. H. Duff (2004), Denitrification and hydrologic transient storage in a glacial meltwater stream, McMurdo Dry Valleys, Antarctica, *Limnol. Oceanogr.*, 49(5), 1884–1895, doi:10.4319/lo.2004.49.5.1884.
- Gooseff, M. N., J. LaNier, R. Haggerty, and K. Kokkeler (2005), Determining in-channel (dead zone) transient storage by comparing solute transport in a bedrock channel-alluvial channel sequence, Oregon, *Water Resour. Res.*, 41, W06014, doi:10.1029/2004WR003513.
- Grimm, N. B., and S. G. Fisher (1984), Exchange between interstitial and surface water: Implications for stream metabolism and nutrient cycling, *Hydrobiologia*, 111(3), 219–228, doi:10.1007/BF00007202.
- Gücker, B., and I. G. Boëchat (2004), Stream morphology controls ammonium retention in tropical headwaters, *Ecology*, 85(10), 2818–2827, doi:10.1890/04-0171.
- Haggerty, R., and P. Reeves (2002), STAMMT-L version 1.0 user's manual, 76 pp., Sandia Natl. Lab, Albuquerque, N. M.
- Haggerty, R., S. M. Wondzell, and M. A. Johnson (2002), Power-law residence time distribution in the hyporheic zone of a 2nd-order mountain stream, *Geophys. Res. Lett.*, 29(13), 1640, doi:10.1029/2002GL014743.
- Haggerty, R., A. Argerich, and E. Marti (2008), Development of a “smart” tracer for the assessment of microbiological activity and sediment-water interaction in natural waters: The resazurin-resorufin system, *Water Resour. Res.*, 44, W00D01, doi:10.1029/2007WR006670.
- Haggerty, R., E. Marti, A. Argerich, D. von Schiller, and N. Grimm (2009), Resazurin as a “smart” tracer for quantifying metabolically active transient storage in stream ecosystems, *J. Geophys. Res.*, 114, G03014, doi:10.1029/2008JG000942.
- Harvey, C. F., and S. M. Gorelick (1995), Temporal moment-generating equations: Modeling transport and mass transfer in heterogeneous aquifers, *Water Resour. Res.*, 31(8), 1895–1911, doi:10.1029/95WR01231.
- Harvey, J. W., and C. C. Fuller (1998), Effect of enhanced manganese oxidation in the hyporheic zone on basin-scale geochemical mass balance, *Water Resour. Res.*, 34(4), 623–636, doi:10.1029/97WR03606.
- Harvey, J. W., and B. J. Wagner (2000), Quantifying hydrologic interactions between streams and their subsurface hyporheic zones, in *Streams and Ground Waters*, edited by P. J. Mulholland and J. B. Jones, pp. 3–44, Academic, San Diego, Calif., doi:10.1016/B978-012389845-6/50002-8.
- Johnson, S. L. (2004), Factors influencing stream temperatures in small streams: substrate effects and a shading experiment, *Can. J. Fish. Aquat. Sci.*, 61, 913–923, doi:10.1139/f04-040.
- Karakashev, D., D. Galabova, and I. Simeonov (2003), A simple and rapid test for differentiation of aerobic from anaerobic bacteria, *World J. Microbiol. Biotechnol.*, 19(3), 233–238, doi:10.1023/A:1023674315047.
- Kasahara, T., and S. M. Wondzell (2003), Geomorphic controls on hyporheic exchange flow in mountain streams, *Water Resour. Res.*, 39(1), 1005, doi:10.1029/2002WR001386.
- Kučera, E. (1965), Contribution to the theory of chromatography: Linear nonequilibrium elution chromatography, *J. Chromatogr.*, 19, 237–248.
- McCutchan, J. H., Jr., W. M. Lewis Jr., and J. F. Saunders III (1998), Uncertainty in the estimation of stream metabolism from open-channel oxygen concentrations, *J. N. Am. Benthol. Soc.*, 17(2), 155–164, doi:10.2307/1467959.
- McNicholl, B. P., J. W. McGrath, and J. P. Quinn (2007), Development and application of a resazurin-based biomass activity test for activated sludge plant management, *Water Res.*, 41, 127–133, doi:10.1016/j.watres.2006.10.002.
- Mulholland, P. J., E. R. Marzolf, J. R. Webster, D. R. Hart, and S. P. Hendricks (1997), Evidence that hyporheic zones increase heterotrophic metabolism and phosphorus uptake in forest streams, *Limnol. Oceanogr.*, 42(3), 443–451, doi:10.4319/lo.1997.42.3.0443.
- Mulholland, P. J., et al. (2001), Inter-biome comparison of factors controlling stream metabolism, *Freshwater Biol.*, 46, 1503–1517, doi:10.1046/j.1365-2427.2001.00773.x.
- Naiman, R. J., and J. R. Sedell (1980), Relationships between metabolic parameters and stream order in Oregon, *Can. J. Fish. Aquat. Sci.*, 37(5), 834–847, doi:10.1139/f80-112.
- Ortiz-Zayas, J. R., W. M. Lewis Jr., J. F. Saunders III, J. H. McCutchan Jr., and F. N. Scatena (2005), Metabolism of a tropical rainforest stream, *J. N. Am. Benthol. Soc.*, 24(4), 769–783, doi:10.1899/03-094.1.
- Payn, R. A., M. N. Gooseff, B. L. McGlynn, K. E. Bencala, and S. M. Wondzell (2009), Channel water balance and exchange with subsurface flow along a mountain headwater stream in Montana, United States, *Water Resour. Res.*, 45, W11427, doi:10.1029/2008WR007644.
- Phanikumar, M. S., I. Aslam, C. Shen, D. T. Long, and T. C. Voice (2007), Separating surface storage from hyporheic retention in natural streams using wavelet decomposition of acoustic Doppler current profiles, *Water Resour. Res.*, 43, W05406, doi:10.1029/2006WR005104.
- Romaní, A. M., A. Butturini, F. Sabater, and S. Sabater (1998), Heterotrophic metabolism in a forest stream sediment: surface versus subsurface zones, *Aquat. Microb. Ecol.*, 16, 143–151, doi:10.3354/ame016143.
- Runkel, R. L. (1998), One dimensional transport with inflow and storage (OTIS): A solute transport model for streams and rivers, *U.S. Geol. Surv. Water Resour. Invest. Rep.*, 98-4018.

- Runkel, R. L. (2002), A new metric for determining the importance of transient storage, *J. N. Am. Benthol. Soc.*, 21(4), 529–543, doi:10.2307/1468428.
- Runkel, R. L. (2007), Toward a transport-based analysis of nutrient spiraling and uptake in streams, *Limnol. Oceanogr. Methods*, 5, 50–62, doi:10.4319/lom.2007.5.50.
- Sardin, M., D. Schweich, F. J. Leij, and M. T. van Genuchten (1991), Modeling the nonequilibrium transport of linearly interacting solutes in porous media: A review, *Water Resour. Res.*, 27(9), 2287–2307, doi:10.1029/91WR01034.
- Schmid, B. H. (2003), Temporal moments routing in streams and rivers with transient storage, *Adv. Water Resour.*, 26(9), 1021–1027, doi:10.1016/S0309-1708(03)00086-1.
- Shaw, E. M. (1994), *Hydrology in Practice*, 3rd ed., Chapman and Hall, London.
- Simon, K. A., C. R. Townsend, J. S. Biggs, and W. B. Bowden (2005), Temporal variation of N and P uptake in 2 New Zealand streams, *J. N. Am. Benthol. Soc.*, 24(1), 1–18, doi:10.1899/0887-3593(2005)024<0001:TVONAP>2.0.CO;2.
- Stream Solute Workshop (1990), Concepts and methods for assessing solute dynamics in stream ecosystems, *J. N. Am. Benthol. Soc.*, 9(2), 95–119, doi:10.2307/1467445.
- Sutton, D. J., Z. J. Kabala, A. Francisco, and D. Vasudevan (2001), Limitations and potential of commercially available rhodamine WT as a groundwater tracer, *Water Resour. Res.*, 37(6), 1641–1656, doi:10.1029/2000WR900295.
- Tank, J. L., E. J. Rosi-Marshall, M. A. Baker, and R. O. Hall (2008), Are rivers just big streams? A pulse method to quantify nitrogen demand in a large river, *Ecology*, 89(10), 2935–2945, doi:10.1890/07-1315.1.
- Triska, F. J., V. C. Kennedy, R. J. Avanzino, G. W. Zellweger, and K. E. Bencala (1989), Retention and transport of nutrients in a third-order stream in Northwestern California: Hyporheic processes, *Ecology*, 70(6), 1893–1905, doi:10.2307/1938120.
- Valett, H. M., J. A. Morrice, and C. N. Dahm (1996), Parent lithology, groundwater-surface water exchange and nitrate retention in headwater streams, *Limnol. Oceanogr.*, 41(2), 333–345, doi:10.4319/lo.1996.41.2.0333.
- Wagner, B. J., and J. W. Harvey (1997), Experimental design for estimating parameters of rate-limited mass transfer: Analysis of stream transfer studies, *Water Resour. Res.*, 33(7), 1731–1741, doi:10.1029/97WR01067.
- Webster, J. R., et al. (2003), Factors affecting ammonium uptake in streams – an inter-biome perspective, *Freshwater Biol.*, 48(8), 1329–1352, doi:10.1046/j.1365-2427.2003.01094.x.
- Wondzell, S. M. (2006), Effect of morphology and discharge on hyporheic exchange flows in two small streams in the Cascade Mountains of Oregon, USA, *Hydrol. Processes*, 20(2), 267–287, doi:10.1002/hyp.5902.
- Wörman, A. (2000), Comparison of models for transient storage of solutes in small streams, *Water Resour. Res.*, 36(2), 455–468, doi:10.1029/1999WR900281.
- Wörman, A., and P. Wachniew (2007), Reach scale and evaluation methods as limitations for transient storage properties in streams and rivers, *Water Resour. Res.*, 43, W10405, doi:10.1029/2006WR005808.
- Young, R. G., and A. D. Huryn (1996), Interannual variation in discharge controls ecosystem metabolism along a grassland river continuum, *Can. J. Fish. Aquat. Sci.*, 53(10), 2199–2211, doi:10.1139/f96-186.
- Zarnetske, J. P., M. N. Gooseff, T. R. Brosten, J. H. Bradford, J. P. McNamara, and W. B. Bowden (2007), Transient storage as a function of geomorphology, discharge, and permafrost active layer conditions in Arctic tundra streams, *Water Resour. Res.*, 43, W07410, doi:10.1029/2005WR004816.

A. Argerich, R. Haggerty, and J. Zarnetske, Department of Geosciences, Oregon State University, 104 Wilkinson Hall, Corvallis, OR 97330, USA. (alba.argerich@gmail.com)

E. Martí, Biogeodynamics and Biodiversity Group, Centre d'Estudis Avançats de Blanes, Accés a la Cala St. Francesc 14, E-17300 Blanes, Spain.

F. Sabater, Departament d'Ecologia, Universitat de Barcelona, Diagonal 645, E-08028 Barcelona, Spain.